Impact of local-moment fluctuations on the magnetic degeneracy of iron arsenide superconductors

Xiaoyu Wang and Rafael M. Fernandes*
School of Physics and Astronomy, University of Minnesota, Minneapolis, Minnesota 55455, USA
(Received 20 December 2013; revised manuscript received 20 March 2014; published 7 April 2014)

We investigate the fate of the orthorhombic stripe-type magnetic state [ordering vectors $(\pi,0)/(0,\pi)$], observed in most iron-pnictide superconductors, in the presence of localized magnetic moments that tend to form a Néel state [ordering vector (π,π)]. We show that before long-range Néel order sets in, the coupling between the conduction electrons and the fluctuations of the local moments favors an unusual magnetic state consisting of a coherent superposition of the $(\pi,0)$ and $(0,\pi)$ orders that preserves tetragonal symmetry. The magnetization of this state is nonuniform and induces a simultaneous checkerboard charge order. We discuss signatures of this magnetic configuration on the electronic spectrum and its impact on the superconducting state, showing that its phase space for coexistence with the s^{+-} state is smaller than the stripe-type state. Our results shed light on recent experimental observations on $Ba(Fe_{1-x}Mn_x)_2As_2$ compounds, where the Néel-type local Mn moments interact with the Fe conduction electrons.

DOI: 10.1103/PhysRevB.89.144502 PACS number(s): 74.70.Xa, 74.20.Mn, 74.25.Ha, 74.40.Kb

I. INTRODUCTION

The proximity between magnetic order and unconventional superconductivity in several materials has been a key motivation to investigate pairing mediated by spin fluctuations [1]. Interestingly, the parent compounds of the two families of high-temperature superconductors, cuprates and iron pnictides, display rather different magnetic ground states. While in the former a Mott insulating Néel-type magnetic configuration [ordering vector $\mathbf{Q}_N = (\pi,\pi)$] is observed, in the latter one finds a metallic stripe-type state [ordering vectors $\mathbf{Q}_1 = (\pi,0)$ or $\mathbf{Q}_2 = (0,\pi)$ in the Fe-square lattice] that breaks the tetragonal symmetry of the system down to orthorhombic. These differences in the magnetic spectra are manifested in the distinct pairing states promoted by the spin fluctuations—*d* wave for the cuprates and s^{+-} for the iron pnictides [2].

To better understand the similarities and differences between these two classes of materials, it is desirable to study a system that interpolates between these two magnetic ground states [3]. Experimentally, a promising material is the $Ba(Fe_{1-x}Mn_x)_2As_2$ compound: for $x = 0$ it undergoes a nearly simultaneous magnetic-structural transition to a metallic stripe-type state at $T_{mag} \approx 137$K [4,5] with a saturated magnetic moment of about $0.9\,\mu_B$ [6]. Optical conductivity [7] and ARPES [8] measurements indicate that the conduction Fe electrons are directly involved in the formation of the magnetic state, in agreement with first-principle calculations [9]. For $x = 1$ the system undergoes a magnetic transition at much higher temperatures, $T_{mag} \approx 625$K, forming an insulating Néel state with a large saturated magnetic moment of $3.9\,\mu_B$ [10–12]. Whether this state is a Mott insulator remains to be seen [13], but both theory and experiment suggest that correlations are stronger than in the $x = 0$ compound [14] and that a local Mn moment picture describes well the ordered state [15–19]. Although no superconductivity has been observed in these compounds, short-range Néel fluctuations, presumably arising from the Mn moments, are observed via neutron scattering even for small doping levels $x \approx 0.07$ [20]. Remarkably, x-ray and neutron diffraction measurements report an unusual intermediate magnetic state for $x \gtrsim 0.1$, which does not break the tetragonal symmetry of the system despite the presence of magnetic Bragg peaks at $\mathbf{Q}_1 = (\pi,0)$ or $\mathbf{Q}_2 = (0,\pi)$ [21].

Theoretically, the transition from a stripe phase to a Néel state may seem at first sight straightforward. In a square-lattice local-moment model with nearest-neighbor and next-nearest-neighbor antiferromagnetic exchanges J_1 and J_2, respectively, there is a classical transition from a stripe to a Néel state once $J_1 > 2J_2$ [22]. However, the fact that the stripe state in the pnictides is metallic, with conduction electrons forming the magnetic moments, opens novel possibilities. This is because the itinerant magnetic state driven by the nesting properties of the Fermi surface is highly degenerate [23–27]: besides the stripe phase, other configurations that do not break tetragonal symmetry, with noncollinear or nonuniform magnetization, may minimize the magnetic free energy (see Fig. 1). The interaction with local moments affects this intricate free-energy landscape and can potentially give rise to unusual magnetic ground states.

In this paper, motivated by the physics of these $Ba(Fe_{1-x}Mn_x)_2As_2$ compounds, we show that short-range Néel-type fluctuations favor a different magnetic state that does not break tetragonal symmetry but that still displays magnetic Bragg peaks at $\mathbf{Q}_1 = (\pi,0)$ and $\mathbf{Q}_2 = (0,\pi)$, in qualitative agreement with the observations in the $x \approx 0.1$ $Ba(Fe_{1-x}Mn_x)_2As_2$ compounds. Its magnetic configuration is nonuniform, inducing a secondary charge density-wave with ordering vector $\mathbf{Q}_N$, which can be detected experimentally. We also determine the changes in the electronic spectrum—which can be probed by ARPES and STM—promoted by this magnetic tetragonal state. The main difference from the reconstructed Fermi surface of the stripe state is the absence of a central unhybridized hole pocket, replaced by additional reconstructed pockets at high-symmetry directions. Finally, we show that the nonuniform state tends to phase-separate from the s^{+-} superconducting state, which helps to explain the absence of coexisting superconductivity in the $Ba(Fe_{1-x}Mn_x)_2As_2$ compounds, in contrast to their $Ba(Fe_{1-x}Co_x)_2As_2$ counterparts.

The paper is organized as follows: in Sec. II we develop a general Ginzburg-Landau model that captures the three

*Corresponding author: rfernand@umn.edu

 ©2014 American Physical Society

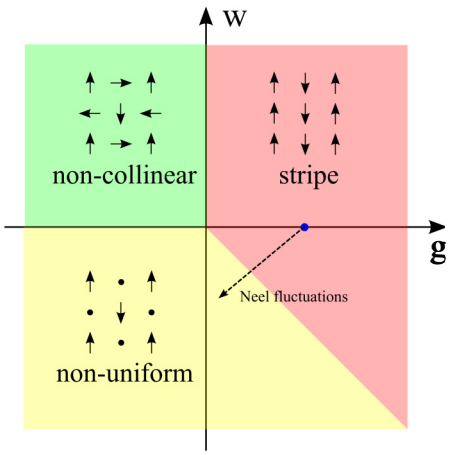

FIG. 1. (Color online) Phase diagram of the Ginzburg-Landau model Eq. (1), displaying the orthorhombic stripe-type state for $g > \max\{0, -w\}$, as well as the tetragonal nonuniform and noncollinear states for $g < \max\{0, -w\}$ (see also Refs. [23,24]). In the absence of Néel fluctuations, the ground state is the stripe one (blue dot). As Néel fluctuations increase, a transition from the stripe to the nonuniform state takes place (dashed arrow).

different possible magnetic ground states of the iron pnictides. In Sec. III we introduce a microscopic model where the itinerant electrons couple to local Néel moments, showing that Néel fluctuations favor the nonuniform tetragonal magnetic state. In Sec. IV we discuss the reconstructed electronic spectrum due to this peculiar order, and in Sec. V, its impact on superconductivity. Section VI is devoted to the concluding remarks.

II. PHENOMENOLOGICAL MODEL: DEGENERACY OF THE MAGNETIC GROUND STATE

The enlarged degeneracy of the itinerant magnetic ground state of the iron pnictides can be captured by a phenomenological Ginzburg-Landau model [23,26,27]. In the tetragonal phase, neutron scattering experiments find magnetic fluctuations of equal amplitude peaked at the two ordering vectors $\mathbf{Q}_1 = (\pi,0)$ and $\mathbf{Q}_2 = (0,\pi)$ [20]. Therefore, we introduce two $O(3)$ magnetic order parameters, $\mathbf{M}_1$ and $\mathbf{M}_2$, associated, respectively, with $\mathbf{Q}_1$ and $\mathbf{Q}_2$. As a result, the spin at position $\mathbf{r}$ is in general a superposition of the two order parameters, i.e., $\mathbf{S}(\mathbf{r}) = \mathbf{M}_1 e^{i\mathbf{Q}_1\cdot\mathbf{r}} + \mathbf{M}_2 e^{i\mathbf{Q}_2\cdot\mathbf{r}}$. The most general free-energy expansion that respects tetragonal and $O(3)$ symmetries is

$$F = \frac{a}{2}\left(M_1^2 + M_2^2\right) + \frac{u}{4}\left(M_1^2 + M_2^2\right)^2 - \frac{g}{4}\left(M_1^2 - M_2^2\right)^2 + w(\mathbf{M}_1\cdot\mathbf{M}_2)^2. \quad (1)$$

The first two terms depend only on the combination $M_1^2 + M_2^2$, effectively enlarging the symmetry of the system to O(6), and resulting in a huge degeneracy of the magnetic ground state [24,25]. The last two terms are responsible for lifting this degeneracy, selecting both the relative amplitudes (either $M_1^2/M_2^2 = 0$ or $M_1^2/M_2^2 = 1$) and the relative orientations of the two order parameters (either $\mathbf{M}_1 \parallel \mathbf{M}_2$ or $\mathbf{M}_1 \perp \mathbf{M}_2$). Figure 1 displays the phase diagram and the resulting ground states as function of g and w. For $g > \max\{0, -w\}$, we find a stripe-type state, characterized by $M_1 \neq 0$ and $M_2 = 0$ (or vice-versa), which breaks the tetragonal symmetry of the system. This is the state most commonly observed in the iron pnictides and has a residual Z_2 (Ising) symmetry, related to choosing either $M_1 \neq 0$ or $M_2 \neq 0$, which can be broken even before the magnetic transition takes place [27].

For $g < \max\{0, -w\}$, minimization of the free energy leads to a tetragonal magnetic state characterized by simultaneously nonvanishing $M_1^2 = M_2^2$. Two different configurations are possible: for $w > 0$, we obtain the noncollinear state $\mathbf{M}_1 \perp \mathbf{M}_2$, where nearest-neighbor spins of amplitude $\langle S_i\rangle = \sqrt{2}M$ are orthogonal to each other (see Fig. 1 and also Refs. [23,24]). For $w < 0$, the ground state is given by $\mathbf{M}_1 \parallel \mathbf{M}_2$, corresponding to a nonuniform collinear state (see Fig. 1 and Refs. [23,24]). In this configuration, odd sites of the original square lattice form a nonmagnetic sublattice, with local spin $\langle S_{i_{\text{odd}}}\rangle = 0$, whereas even sites form a Néel sublattice, with $\langle S_{i_{\text{even}}}\rangle = 2M$. This nonuniform state induces a charge density-wave (CDW) with modulation $\mathbf{Q}_1 + \mathbf{Q}_2 = \mathbf{Q}_N$, where the odd (nonmagnetic) sites have different local charge than the even (magnetic) sites. This can be obtained from Eq. (1) by including the charge degrees of freedom [28]:

$$\tilde{F} = F - \zeta\,\rho_{\mathbf{Q}_N}(\mathbf{M}_1\cdot\mathbf{M}_2) + \frac{1}{2}\,\chi_{\text{CDW}}^{-1}\rho_{\mathbf{Q}_N}^2. \quad (2)$$

Here, $\rho_{\mathbf{Q}_N}$ is the Fourier component of the charge density $\rho(\mathbf{r})$ at momentum $\mathbf{Q}_N = (\pi,\pi)$; i.e., it is related to a checkerboard charge-density wave. Minimization with respect to the CDW order parameter gives $\rho_{\mathbf{Q}_N} = \chi_{\text{CDW}}\zeta\,(\mathbf{M}_1\cdot\mathbf{M}_2)$, implying that its amplitude in the magnetically ordered state depends on both the coupling constant ζ and the bare CDW susceptibility χ_{CDW}.

The vast majority of iron pnictides display a stripe-type ground state, $g > \max\{0, -w\}$. The recent observation in the $Ba(Fe_{1-x}Mn_x)_2As_2$ compounds of a magnetic state with peaks at $\mathbf{Q}_1 = (\pi,0)$ and $\mathbf{Q}_2 = (0,\pi)$ but no orthorhombic distortion [21] indicates that upon sufficient Mn doping, the Ginzburg-Landau coefficients change and bring the system to the regime of tetragonal magnetic states (either the nonuniform or the noncollinear state). Our goal now is to develop a microscopic model to evaluate these coefficients and unveil the mechanism behind these changes.

III. MICROSCOPIC MODEL: IMPACT OF NÉEL FLUCTUATIONS

The typical Fermi surface of the iron pnictides is shown in Fig. 3(a), obtained from the tight-binding model of Ref. [29]. To make our analysis more transparent, we follow Refs. [24,27] and consider an effective model with a (possibly degenerate) circular hole pocket h at the center of the Brillouin zone and two elliptical electron pockets $e_{1,2}$ centered at $\mathbf{Q}_1 = (\pi,0)$ and $\mathbf{Q}_2 = (0,\pi)$. The band dispersions are, respectively,

$$\varepsilon_{h,\mathbf{k}} = \epsilon_0 - \frac{k^2}{2m} - \mu$$

$$\varepsilon_{e_1,\mathbf{k}+\mathbf{Q}_1} = -\epsilon_0 + \frac{k_x^2}{2m_x} + \frac{k_y^2}{2m_y} - \mu$$

$$\varepsilon_{e_2,\mathbf{k}+\mathbf{Q}_2} = -\epsilon_0 + \frac{k_x^2}{2m_y} + \frac{k_y^2}{2m_x} - \mu.$$

Close to particle-hole symmetry (perfect nesting), we can rewrite the band dispersions in a more convenient form:

$$\begin{aligned}\varepsilon_{h,\mathbf{k}} &= -\varepsilon_{\mathbf{k}}\\ \varepsilon_{e_1,\mathbf{k}+\mathbf{Q}_1} &= \varepsilon_{\mathbf{k}} - (\delta_\mu + \delta_m \cos 2\theta)\\ \varepsilon_{e_2,\mathbf{k}+\mathbf{Q}_2} &= \varepsilon_{\mathbf{k}} - (\delta_\mu - \delta_m \cos 2\theta),\end{aligned} \tag{3}$$

where θ is the angle around the Fermi surface. The parameter δ_μ is related to the occupation number (doping), and δ_m is related to the ellipticity of the electron pockets:

$$\begin{aligned}\delta_\mu &= 2\mu + \epsilon_F\left[1 - \frac{m}{2}\left(\frac{m_x + m_y}{m_x m_y}\right)\right],\\ \delta_m &= \frac{\epsilon_F m}{2}\left(\frac{m_x - m_y}{m_x m_y}\right),\end{aligned} \tag{4}$$

where ϵ_F is the Fermi energy. Thus, the noninteracting Hamiltonian is given by $H_0 = \sum_{\mathbf{k},a} \varepsilon_{\mathbf{k},a} c^\dagger_{a,\mathbf{k}\alpha} c_{a,\mathbf{k}\alpha}$, with band index a and spin index α. Projecting the interacting Hamiltonian in the SDW channel [30]—which is the leading instability of the system—yields the term $H_I = U_{\mathrm{SDW}} \sum_{\mathbf{q},i} \mathbf{s}^{(i)}_{\mathbf{q}} \cdot \mathbf{s}^{(i)}_{-\mathbf{q}}$, where $\mathbf{s}^{(i)}_{\mathbf{q}} = \sum_{\mathbf{k}} c^\dagger_{h,\mathbf{k}+\mathbf{q}\alpha} \boldsymbol{\sigma}_{\alpha\beta} c_{e_i,\mathbf{k}+\mathbf{Q}_i\beta}$ are the two staggered spin operators whose mean values are proportional to the two order parameters $\mathbf{M}_i$.

The free energy Eq. (1) can now be *derived* from the total Hamiltonian $H_0 + H_I$ by performing Hubbard-Stratonovich transformations and integrating out the electronic degrees of freedom [27]. We consider $\mathbf{M}_i$ to be real and homogeneous. The Ginzburg-Landau coefficients, as obtained in Ref. [27], are given by $w = 0$ and

$$u = \int_k G^2_{h,k}(G_{e_1,k} + G_{e_2,k})^2 \approx \frac{7\zeta(3)\rho_F}{2\pi^2 T^2}, \tag{5}$$

$$g = -\int_k G^2_{h,k}(G_{e_1,k} - G_{e_2,k})^2 \approx \frac{31\zeta(5)\rho_F}{32\pi^4 T^2}\left(\frac{\delta_m}{T}\right)^2, \tag{6}$$

where $G^{-1}_{a,k} = i\omega_n - \varepsilon_{a,\mathbf{k}}$ are the noninteracting single-particle Green's functions, and ρ_F is the density of states at the Fermi level. In the limit of perfect nesting (i.e., $\delta_\mu = \delta_m = 0$) one obtains $g = w = 0$, implying that the system has an enlarged O(6) symmetry and a huge ground-state degeneracy. Expanding near-perfect nesting yields $g \propto \delta_m^2 > 0$ and $w = 0$, placing the system in the regime of a stripe-type magnetic state (blue dot in Fig. 1). Similar free-energy calculations considering other types of band dispersions also find that the stripe state is favored for a wide range of parameters, consistent with the observations that most iron pnictides display this magnetic ordered state [23,26,31,32].

To make contact with the $Ba(Fe_{1-x}Mn_x)_2As_2$ compounds, we include the coupling between the conduction electrons and Néel-type fluctuations. As shown by first-principle and model calculations, Néel fluctuations are always present in the iron pnictides due to the existence of two matching electron pockets separated by $\mathbf{Q}_N = (\pi,\pi)$ [31,33,34]. The presence of Mn dopants enhances these fluctuations, because the magnetic Mn dopants promote Néel order—indeed, the "fully doped" $BaMn_2As_2$ compound displays a transition to a Néel magnetic state at rather high temperatures [10]. The coupling between the local Mn moments and the Fe conduction electrons is attested by local probes such as ESR (electron spin resonance) [35] and NMR (nuclear magnetic resonance) [16]. This unique behavior of the Mn dopants should be contrasted with other types of chemical substitution in the Fe site, $Ba(Fe_{1-x}M_x)_2As_2$, such as $M =$ Co, Ni, Cu. For instance, Co and Ni are nonmagnetic, as shown by ESR measurements [35]. Cu, although magnetic, does not seem to favor a Néel state, since the "fully doped" $BaCu_2As_2$ compound remains paramagnetic [36,37].

Experimental evidence for Néel fluctuations in $Ba(Fe_{1-x}Mn_x)_2As_2$ is given by neutron diffraction experiments, which observe an inelastic magnetic peak at $\mathbf{Q}_N = (\pi,\pi)$ already for very small Mn-doping levels x [20], where no long-range Néel order is observed. In this dilute limit, Mn dopants are also expected to promote impurity scattering. One of its main effects is to suppress the magnetic transition temperature T_{mag}, as discussed in Refs. [38,39]. Within our model, T_{mag} appears in the quadratic term of the general Ginzburg-Landau expansion in Eq. (1), and therefore is not responsible for the selection of the ground state—which is determined solely by the quartic coefficients. Thus, hereafter we focus only on the role played by Néel fluctuations. Denoting by $\mathbf{N}$ the collective field associated with these Néel fluctuations, and by $\chi_N(\mathbf{q})$ the corresponding momentum-dependent susceptibility, we therefore consider the coupling between the Néel fluctuations and the itinerant electrons according to Ref. [34]:

$$H_N = \sum_{\mathbf{k}} \mathbf{N} \cdot (c^\dagger_{e_1,\mathbf{k}+\mathbf{Q}_1\alpha} \boldsymbol{\sigma}_{\alpha\beta} c_{e_2,\mathbf{k}+\mathbf{Q}_2\beta}), \tag{7}$$

where, for simplicity, the coupling constant was incorporated to $\mathbf{N}$. To determine how the magnetic ground state is affected by short-range Néel fluctuations, we rederive the coefficients of the free energy Eq. (1) from the Hamiltonian $H_0 + H_I + H_N$, expanding to the leading quadratic order in $\mathbf{N}$:

$$\begin{aligned}\delta F = {}& \frac{\alpha}{2} N^2\left(M_1^2 + M_2^2\right) - 4\lambda_{12}[(\mathbf{M}_1 \times \mathbf{M}_2)\cdot\mathbf{N}]^2\\ &+ \left(\frac{4\lambda_{11} + 8\lambda_{12}}{4}\right) N^2\left(M_1^2 + M_2^2\right)^2\\ &- \left(-\frac{4\lambda_{11} + 8\lambda_{12}}{4}\right) N^2\left(M_1^2 - M_2^2\right)^2,\end{aligned} \tag{8}$$

with the coefficients

$$\begin{aligned}\alpha &= 4\int_k G_{h,k} G^2_{e_1,k} G_{e_2,k}\\ \lambda_{ij} &= \int_k G^2_{h,k} G_{e_1,k} G_{e_2,k} G_{e_i,k} G_{e_j,k}.\end{aligned} \tag{9}$$

The coefficients λ_{ij} are represented diagrammatically in Fig. 2(a). Near-perfect nesting, $\alpha > 0$, which reflects the competition between the Néel and stripe states. To study the corrections to the quartic terms of Eq. (1), denoted here by a tilde, we consider Gaussian isotropic Néel fluctuations $\langle N_i N_j\rangle = \frac{\langle N^2\rangle}{3}\delta_{ij}$ and evaluate the diagrams close to perfect

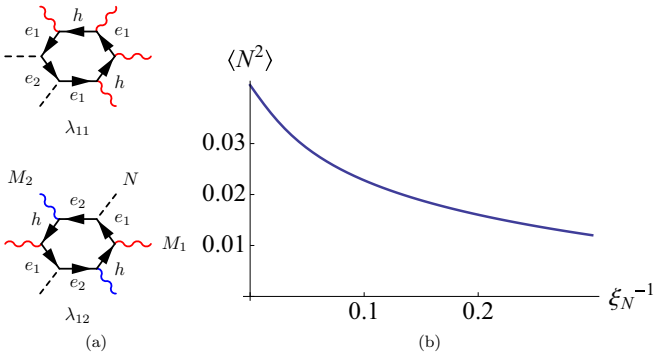

FIG. 2. (Color online) (a) Feynman diagrams λ_{ij} associated with the coupling between the Néel collective field $\mathbf{N}$ (dashed lines) and the magnetic order parameters $\mathbf{M}_1$ and $\mathbf{M}_2$ (wavy lines). The solid (black) lines are the Green's functions of the corresponding bands. (b) Behavior of the Gaussian Néel fluctuations $\langle N^2\rangle$ as function of the inverse Néel correlation length ξ_N^{-1}. The Néel critical point is at $\xi_N^{-1} = 0$.

nesting, obtaining

$$\frac{\tilde{u}}{u} \approx 1 - 0.13\,\frac{\langle N^2\rangle}{T_0^2}$$
$$\frac{\tilde{g}}{u} \approx 0.024\left(\frac{\delta_m^2}{T_0^2} - \frac{4\langle N^2\rangle}{3T_0^2}\right)$$
$$\frac{\tilde{w}}{u} \approx -0.016\,\frac{\langle N^2\rangle}{T_0^2}, \qquad (10)$$

where T_0 is the energy scale of the bare magnetic transition temperature. Thus, when Néel fluctuations are strong enough compared to the energy scale of the ellipticity of the electron pockets, $\langle N^2\rangle > \delta_m^2/2$, the leading instability of the system is toward the nonuniform magnetic state ($0 < \tilde{g} < -\tilde{w}$), which preserves the tetragonal symmetry of the system and induces a simultaneous checkerboard charge order. Notice that, in the Gaussian approximation, $\langle N^2\rangle \propto \int_{\mathbf{q}} \chi_N(\mathbf{q})$ does not diverge at the Néel critical point [see Fig. 2(b)], so this nonuniform magnetic state is not guaranteed to appear (see also Appendix).

The possible existence of this intermediate state between an itinerant stripe-type state and a localized Néel phase is the main result of this paper. We note that a similar result also holds when the Néel instability takes place at temperatures higher than the one where the conduction electrons order magnetically, i.e., where $N^2 \to \langle N\rangle^2$. Note also that this approximation breaks down near the critical region of the Néel transition, where higher-order terms may be necessary.

IV. EXPERIMENTAL MANIFESTATIONS: RECONSTRUCTED ELECTRONIC SPECTRUM

The most prominent experimental signature of the nonuniform state is the absence of orthorhombic distortion (i.e., no splitting of the lattice Bragg peaks) and the presence of magnetic Bragg peaks at $\mathbf{Q}_1 = (\pi,0)$ and $\mathbf{Q}_2 = (0,\pi)$. Indeed, this is what x-ray and neutron diffraction experiments find in the $Ba(Fe_{1-x}Mn_x)_2As_2$ compounds for $x \gtrsim 0.1$ [21]. However, these features are also consistent with the noncollinear state. This is the ground state when $g < 0$—which may in fact be accomplished by the Néel fluctuations, see Eq. (10)—and $w > 0$, which would require other mechanisms than Néel fluctuations [40]. The key property that distinguishes between the nonuniform and noncollinear tetragonal magnetic states is the existence of an induced checkerboard charge order in the former, $\rho_{\mathbf{Q}_N} \propto \mathbf{M}_1 \cdot \mathbf{M}_2$. Because $\mathbf{Q}_N$ coincides with a Bragg peak of the two-Fe unit cell, detecting this secondary order via x-ray may be challenging. However, local probes such as STM could detect this type of charge order. NMR could also distinguish the nonuniform and noncollinear states, since in the former half of the sites display zero averaged magnetization, while in the latter every site is magnetic.

We emphasize that magnetic Bragg peaks at both momenta $\mathbf{Q}_1 = (\pi,0)$ and $\mathbf{Q}_2 = (0,\pi)$ are also expected in the stripe state, due to the formation of domains. This makes it difficult to distinguish between the stripe and nonuniform states using only neutron diffraction data. Furthermore, relying only on the absence of orthorhombic distortion to make this distinction could be an issue depending on the limitations imposed by the x-ray experimental resolution—see for instance Refs. [41,42]. In this regard, absence of shear modulus softening above $T_{\rm mag}$ would provide strong evidence for a tetragonal magnetic state [43–46]. Alternatively, the properties of the electronic spectrum in the magnetic state could be used to differentiate between the stripe and nonuniform states.

To obtain the reconstructed Fermi surface in the nonuniform and striped states, we start with the five-orbital tight-binding model of Ref. [29], with the Hamiltonian

$$H_0 = \sum_{mn}\sum_{\mathbf{k}\sigma} c^\dagger_{m,\mathbf{k}\sigma}(t_{mn} + \epsilon_m\delta_{mn} - \mu\delta_{mn})c_{n,\mathbf{k}\sigma}, \qquad (11)$$

where σ is the spin index, and $m,n = 1...5$ label the five d orbitals of the Fe atom. t_{mn},ϵ_m are the hopping parameters and onsite energies given in Ref. [29]. The chemical potential is $\mu = 0$ for the undoped compound, corresponding to an occupation number of $n = 6$.

The presence of nonzero magnetic order parameters $\mathbf{M}_1$ and $\mathbf{M}_2$ gives rise to to the term

$$H_{\rm mag} = \sum_{i=1,2}\sum_{m}\sum_{\mathbf{k}\alpha\beta} c^\dagger_{m,\mathbf{k}\alpha}(\mathbf{M}_i\cdot\boldsymbol{\sigma}_{\alpha\beta})c_{m,\mathbf{k}+\mathbf{Q}_i,\beta}$$
$$+\kappa\sum_{m}\sum_{\mathbf{k}\alpha} c^\dagger_{m,\mathbf{k}\alpha}(\mathbf{M}_1\cdot\mathbf{M}_2)c_{m,\mathbf{k}+\mathbf{Q}_1+\mathbf{Q}_2,\alpha} + \text{H.c.}, \qquad (12)$$

where we considered only intraorbital magnetic order parameters [47], assumed for simplicity to be of equal amplitude. κ is a coupling constant that determines the amplitude of the higher-order harmonic generated when both $\mathbf{M}_1$ and $\mathbf{M}_2$ are nonzero—which gives rise to the checkerboard charge order. In our calculations, we found that the reconstructed Fermi surface does not depend strongly on the choice of κ.

The reconstructed band structure for the stripe and nonuniform orders can be obtained by diagonalizing the full Hamiltonian $H = H_0 + H_{\rm mag}$ adjusting the chemical potential μ under the constraint of fixed occupation number $n = 6$. To diagonalize the Hamiltonian, we introduce the Nambu

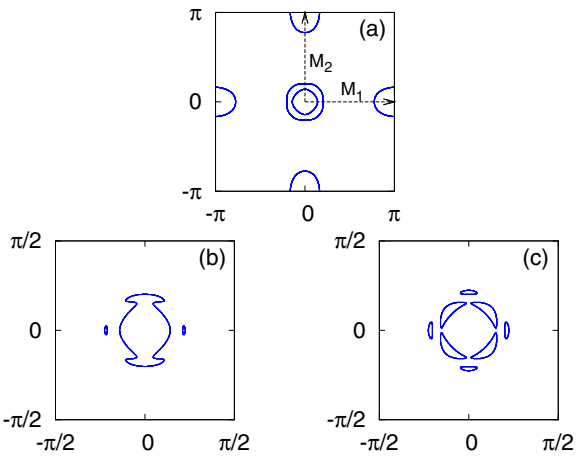

FIG. 3. (Color online) Reconstructed Fermi surfaces near the center of the Brillouin zone in the presence of $\mathbf{Q}_1 = (\pi,0)$ stripe-type magnetic order (b) and nonuniform magnetic order (c). The Fermi surface in the paramagnetic state is shown in (a), with the tight-binding parameters of Ref. [29].

operators:

$$\psi^\dagger_{m,\mathbf{k}\sigma} = (c^\dagger_{m,\mathbf{k}\sigma} \quad c^\dagger_{m,\mathbf{k}+\mathbf{Q}_1\sigma} \quad c^\dagger_{m,\mathbf{k}+\mathbf{Q}_2\sigma} \quad c^\dagger_{m,\mathbf{k}+\mathbf{Q}_1+\mathbf{Q}_2\sigma}).$$

The order parameters couple different elements in Nambu space: $\mathbf{M}_i$ couples $c^\dagger_{m,\mathbf{k}\sigma}$ to $c_{m,\mathbf{k}+\mathbf{Q}_i\sigma'}$ and $c^\dagger_{m,\mathbf{k}+\mathbf{Q}_i\sigma}$ to $c_{m,\mathbf{k}+\mathbf{Q}_1+\mathbf{Q}_2\sigma'}$, while $\mathbf{M}_1 \cdot \mathbf{M}_2$ couples $c^\dagger_{m,\mathbf{k}+\mathbf{Q}_1\sigma}$ to $c_{m,\mathbf{k}+\mathbf{Q}_2\sigma'}$ and $c^\dagger_{m,\mathbf{k}\sigma}$ to $c_{m,\mathbf{k}+\mathbf{Q}_1+\mathbf{Q}_2\sigma'}$. For the $(\pi,0)$ stripe order, $\mathbf{M}_2 = 0$ and $\mathbf{M}_1 = M\hat{\mathbf{x}}$, and the magnetic unit cell is given by $-\pi/2 \leqslant k_x \leqslant \pi/2$ and $-\pi \leqslant k_y \leqslant \pi$. For the nonuniform magnetic order, $\mathbf{M}_1 = \mathbf{M}_2 = \frac{M}{\sqrt{2}}\hat{x}$, where the factor of $\sqrt{2}$ is introduced to keep the total order parameter $\sqrt{M_1^2 + M_2^2}$ the same as in the striped case. The magnetic unit cell is given in this case by $-\pi/2 \leqslant k_x, k_y \leqslant \pi/2$.

In Fig. 3, we present the reconstructed Fermi surface around the center of the magnetic Brillouin zone for both magnetic ground states. In the paramagnetic phase, the Fermi surface consists of two concentric hole pockets at the center of the Brillouin zone and two elliptical pockets centered at the momenta $\mathbf{Q}_1 = (\pi,0)$ and $\mathbf{Q}_2 = (0,\pi)$. In the striped state, we find that for reasonable values of the magnetic order parameter ($M \approx 60$ meV), one of the hole pockets remains unhybridized while the other hole pocket hybridizes with the folded electron pocket, giving rise to "Dirac cones"—the small reconstructed pockets along the stripe modulation direction. This is in general agreement with previous theoretical and experimental results [47–49]. On the other hand, for the nonuniform state, each of the two hole pockets hybridize with one of the two electron pockets. As a result, there remains only small reconstructed pockets [50]. Unlike the small pockets that appear in the stripe state case, four of these pockets appear along the $\mathbf{Q}_1 + \mathbf{Q}_2 = (\pi,\pi)$ direction, a unique signature of the double-$\mathbf{Q}$ nonuniform magnetic order.

V. COEXISTENCE BETWEEN TETRAGONALLY SYMMETRIC MAGNETISM AND SUPERCONDUCTIVITY

An intriguing observation in the $Ba(Fe_{1-x}Mn_x)_2As_2$ compounds is the absence of superconductivity, despite the fact that the magnetic transition is suppressed down to 50 K. In the closely related compounds $Ba(Fe_{1-x}Co_x)_2As_2$, for instance, one observes coexistence between superconductivity and magnetism for similar values of $T_{\rm mag}$ [51]. It has been pointed out that the Néel fluctuations in $Ba(Fe_{1-x}Mn_x)_2As_2$ effectively suppress the leading s^{+-} pairing instability and instead promote d-wave pairing [34]. Besides this effect, the possible change in the magnetic ground state also has an impact on the outcome of the competition between long-range magnetic order and superconductivity.

Within the phenomenological model Eq. (1), this competition is described by the additional Ginzburg-Landau terms:

$$\tilde{F} = F + F_{SC} + \frac{\gamma}{2}\Delta^2\left(M_1^2 + M_2^2\right), \tag{13}$$

where Δ is the superconducting order parameter and $\gamma > 0$ is a coupling constant that can be derived directly from the microscopic Hamiltonian $H_0 + H_I$ [52,53]. The superconducting free energy is given by the usual form:

$$F_{\rm SC} = \frac{a_s}{2}\Delta^2 + \frac{u_s}{4}\Delta^4, \tag{14}$$

with $a_s \propto T - T_c$ and $u_s > 0$. To determine whether long-range magnetic order and superconductivity can coexist, we minimize the free energy Eq. (13) with respect to Δ and check whether the renormalized quartic coefficient of M is positive. In general, coexistence takes place when $\frac{\gamma}{\sqrt{u_s}} < \sqrt{\tilde{u}_m}$, where the effective parameter $\tilde{u}_m$ is given by $\tilde{u}_m = \tilde{u} - \tilde{g}$ for the striped state and $\tilde{u}_m = \tilde{u} - |\tilde{w}|$ for the nonuniform state. Using our results from Eq. (10), we plot in Fig. 4 the value of this effective parameter $\tilde{u}_m$ as a function of the amplitude of the Néel fluctuations for both stripe and nonuniform

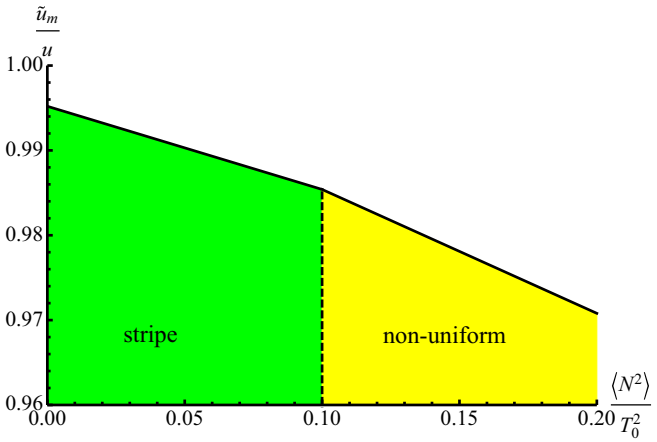

FIG. 4. (Color online) Effective quartic magnetic coefficient $\tilde{u}_m$ as function of the amplitude of Néel fluctuations $\langle N^2\rangle$. The condition for coexistence between superconductivity and long-range magnetism is $\frac{\gamma}{\sqrt{u_s}} < \sqrt{\tilde{u}_m}$, implying that the phase space for the coexistence state is reduced as Néel fluctuations become stronger. In this plot we used $\frac{\delta_m^2}{T_0^2} = 0.2$.

magnetic states. As shown in the Fig. 4, $\tilde{u}_m$ decreases as Néel fluctuations become stronger, restricting the phase space for which coexistence between superconductivity and long-range magnetism is achieved, $\frac{\gamma}{\sqrt{u_s}} < \sqrt{\tilde{u}_m}$. Therefore, stronger Néel fluctuations make it difficult for a coexistence state with either stripe or nonuniform states to be realized.

VI. CONCLUDING REMARKS

In summary, we have shown that an unusual nonuniform tetragonal magnetic state consisting of a coherent combination of $\mathbf{Q}_1 = (\pi,0)$ and $\mathbf{Q}_2 = (0,\pi)$ orders can be realized in the iron pnictides as a result of the interplay between itinerant magnetism promoted by the nesting features of the Fermi surface and Néel-type fluctuations promoted by local moments. This nonuniform state induces a checkerboard charge order and a reconstruction of the electronic spectrum, both of which can be detected experimentally. We argue that our findings may explain the experimental observation of a tetragonal magnetic state displaying Bragg peaks at $\mathbf{Q}_1 = (\pi,0)$ and $\mathbf{Q}_2 = (0,\pi)$ in doped $Ba(Fe_{1-x}Mn_x)_2As_2$, as well as the absence of coexisting superconductivity in these compounds. Besides $Ba(Fe_{1-x}Mn_x)_2As_2$, a tetragonal magnetic state has also been reported in $(Ba_{1-x}Na)Fe_2As_2$ [54], and possibly in 122 compounds under pressure [55,56], but whether Néel fluctuations are also present in these systems remains to be seen. The existence of such tetragonal magnetic states also imposes important constraints on the mechanism of magnetism in the iron pnictides, as they imply that tetragonal symmetry breaking is not a necessary condition to achieve long-range magnetic order.

ACKNOWLEDGMENTS

We thank A. Chubukov, I. Eremin, A. Goldman, J. Knolle, A. Kreyssig, R. McQueeney, A. Millis, J. Schmalian, and G. Tucker for fruitful discussions.

APPENDIX: GAUSSIAN NÉEL FLUCTUATIONS

Here we show how $\langle N^2 \rangle$ is obtained within a Gaussian approximation. The action for the Néel field $\mathbf{N}$ can be written as

$$S_{\text{Néel}}[\mathbf{N}] = \frac{1}{2}\int_q \chi^{-1}_{N,q} N^2 + \int_x \frac{u}{4} N^4, \tag{A1}$$

where $q = (\boldsymbol{q}, \nu_n)$ denotes both momentum and bosonic Matsubara frequency $\nu_n = 2\pi n T$, and $x = (\boldsymbol{r}, \tau)$. For a classical transition in a strongly anisotropic system, the Néel susceptibility takes the form

$$\chi^{-1}_{N,q} = r_0 + q_\parallel^2 + \eta_z \sin^2 q_z, \tag{A2}$$

where $r_0 \propto T - T_{\text{Néel}}$ and η_z is the interplane coupling. Following Ref. [26], the quartic term can be decoupled by an auxiliary field ψ:

$$S_{\text{eff}}[\mathbf{N},\psi] = \frac{1}{2}\int_q \chi_q^{-1} N^2 - \int_x \frac{1}{4u}\psi^2 + \frac{1}{2}\int_x \psi N^2. \tag{A3}$$

Minimization with respect to ψ gives $\langle N^2 \rangle = \langle \psi \rangle / u$. In the absence of long-range Néel order, the $\mathbf{N}$ field can be directly integrated out, yielding the effective action:

$$S_{\text{eff}} = -\frac{\psi^2}{4u} + \frac{3}{2}\int_q \ln\left(\chi_q^{-1} + \psi\right). \tag{A4}$$

Minimization with respect to ψ gives

$$\psi = 3u \int_q \frac{1}{\chi_q^{-1} + \psi}. \tag{A5}$$

Explicit evaluation then yields

$$\psi = \bar{u} \ln \frac{2\Lambda}{\sqrt{r_0 + \psi} + \sqrt{r_0 + \psi + \eta_z}}, \tag{A6}$$

where $\bar{u} = 3uT/(2\pi)$, and Λ is the upper cutoff. In Fig. 2(b) of the paper, the parameters used were $\bar{u}/\Lambda^2 = 0.01$ and $\eta_z/\Lambda^2 = 0.001$. The correlation length is given by $\xi_N = (r_0 + \psi)^{-1/2}$ and diverges at the Néel transition.

[1] D. J. Scalapino, Rev. Mod. Phys. **84**, 1383 (2012).
[2] P. J. Hirschfeld, M. M. Korshunov, and I. I. Mazin, Rep. Prog. Phys. **74**, 124508 (2011); A. V. Chubukov, Annu. Rev. Cond. Mat. Phys. **3**, 57 (2012).
[3] J. W. Simonson, Z. P. Yin, M. Pezzoli, J. Guo, J. Liu, K. Post, A. Efimenko, N. Hollmann, Z. Hu, H.-J. Lin, C. T. Chen, C. Marques, V. Leyva, G. Smith, J. W. Lynn, L. Sun, G. Kotliar, D. N. Basov, L. H. Tjeng, and M. C. Aronson, Proc. Natl. Acad. Sci. U.S.A. **109**, E1815 (2012).
[4] M. G. Kim, R. M. Fernandes, A. Kreyssig, J. W. Kim, A. Thaler, S. L. Bud'ko, P. C. Canfield, R. J. McQueeney, J. Schmalian, and A. I. Goldman, Phys. Rev. B **83**, 134522 (2011).
[5] C. R. Rotundu and R. J. Birgeneau, Phys. Rev. B **84**, 092501 (2011).
[6] K. Ishida, Y. Nakai, and H. Hosono, J. Phys. Soc. Japan **78**, 062001 (2009); D. C. Johnston, Adv. Phys. **59**, 803 (2010); J. Paglione and R. L. Greene, Nature Phys. **6**, 645 (2010); P. C. Canfield and S. L. Bud'ko, Annu. Rev. Cond. Mat. Phys. **1**, 27 (2010); H. H. Wen and S. Li, *ibid.* **2**, 121 (2011).
[7] M. Nakajima, S. Ishida, K. Kihou, Y. Tomioka, T. Ito, Y. Yoshida, C. H. Lee, H. Kito, A. Iyo, H. Eisaki, K. M. Kojima, and S. Uchida, Phys. Rev. B **81**, 104528 (2010).
[8] C. Liu, T. Kondo, R. M. Fernandes, A. D. Palczewski, E. D. Mun, N. Ni, A. N. Thaler, A. Bostwick, E. Rotenberg, J. Schmalian, S. L. Bud'ko, P. C. Canfield, and A. Kaminski, Nature Phys. **6**, 419 (2010).
[9] O. K. Andersen and L. Boeri, Ann. Phys. **523**, 8 (2011).
[10] Y. Singh, A. Ellern, and D. C. Johnston, Phys. Rev. B **79**, 094519 (2009).
[11] J. An, A. S. Sefat, D. J. Singh, and M. H. Du, Phys. Rev. B **79**, 075120 (2009).

[12] A. Pandey, R. S. Dhaka, J. Lamsal, Y. Lee, V. K. Anand, A. Kreyssig, T. W. Heitmann, R. J. McQueeney, A. I. Goldman, B. N. Harmon, A. Kaminski, and D. C. Johnston, Phys. Rev. Lett. **108**, 087005 (2012).

[13] T. Misawa, K. Nakamura, and M. Imada, Phys. Rev. Lett. **108**, 177007 (2012).

[14] Y. X. Yao, J. Schmalian, C. Z. Wang, K. M. Ho, and G. Kotliar, Phys. Rev. B **84**, 245112 (2011).

[15] D. C. Johnston, R. J. McQueeney, B. Lake, A. Honecker, M. E. Zhitomirsky, R. Nath, Y. Furukawa, V. P. Antropov, and Y. Singh, Phys. Rev. B **84**, 094445 (2011).

[16] Y. Texier, Y. Laplace, P. Mendels, J. T. Park, G. Friemel, D. L. Sun, D. S. Inosov, C. T. Lin, and J. Bobroff, Europhys. Lett. **99**, 17002 (2012).

[17] X. Ma, J. Bai, Z. Li, J. Wan, H. Pang, and F. Li, J. Phys.: Condens. Matter **25**, 135703 (2013).

[18] R. Frankovsky, H. Luetkens, F. Tambornino, A. Marchuk, G. Pascua, A. Amato, H.-H. Klauss, and D. Johrendt, Phys. Rev. B **87**, 174515 (2013).

[19] H. Suzuki, T. Yoshida, S. Ideta, G. Shibata, K. Ishigami, T. Kadono, A. Fujimori, M. Hashimoto, D. H. Lu, Z.-X. Shen, K. Ono, E. Sakai, H. Kumigashira, M. Matsuo, and T. Sasagawa, Phys. Rev. B **88**, 100501(R) (2013).

[20] G. S. Tucker, D. K. Pratt, M. G. Kim, S. Ran, A. Thaler, G. E. Granroth, K. Marty, W. Tian, J. L. Zarestky, M. D. Lumsden, S. L. Bud'ko, P. C. Canfield, A. Kreyssig, A. I. Goldman, and R. J. McQueeney, Phys. Rev. B **86**, 020503(R) (2012).

[21] M. G. Kim, A. Kreyssig, A. Thaler, D. K. Pratt, W. Tian, J. L. Zarestky, M. A. Green, S. L. Bud'ko, P. C. Canfield, R. J. McQueeney, and A. I. Goldman, Phys. Rev. B **82**, 220503(R) (2010).

[22] P. Chandra, P. Coleman, and A. I. Larkin, Phys. Rev. Lett. **64**, 88 (1990).

[23] J. Lorenzana, G. Seibold, C. Ortix, and M. Grilli, Phys. Rev. Lett. **101**, 186402 (2008).

[24] I. Eremin and A. V. Chubukov, Phys. Rev. B **81**, 024511 (2010).

[25] J. Kang and Z. Tesanovic, Phys. Rev. B **83**, 020505 (2011).

[26] P. M. R. Brydon, J. Schmiedt, and C. Timm, Phys. Rev. B **84**, 214510 (2011).

[27] R. M. Fernandes, A. V. Chubukov, J. Knolle, I. Eremin, and J. Schmalian, Phys. Rev. B **85**, 024534 (2012).

[28] A. V. Balatsky, D. N. Basov, and J.-X. Zhu, Phys. Rev. B **82**, 144522 (2010).

[29] S. Graser, T. A. Maier, P. J. Hirschfeld, and D. J. Scalapino, New J. Phys. **11**, 025016 (2009).

[30] S. Maiti and A. V. Chubukov, Phys. Rev. B **82**, 214515 (2010).

[31] M. J. Calderón, G. León, B. Valenzuela, and E. Bascones, Phys. Rev. B **86**, 104514 (2012).

[32] Q. Luo and E. Dagotto, Phys. Rev. B **89**, 045115 (2014).

[33] M. D. Johannes and I. I. Mazin, Phys. Rev. B **79**, 220510(R) (2009).

[34] R. M. Fernandes and A. J. Millis, Phys. Rev. Lett. **110**, 117004 (2013).

[35] P. F. S. Rosa, T. M. Garitezi, C. Adriano, T. Grant, Z. Fisk, R. R. Urbano, R. M. Fernandes, and P. G. Pagliuso, J. Appl. Phys. **115**, 17D702 (2014); P. F. S. Rosa *et al*. (unpublished).

[36] D. J. Singh, Phys. Rev. B **79**, 153102 (2009).

[37] V. K. Anand, P. K. Perera, A. Pandey, R. J. Goetsch, A. Kreyssig, and D. C. Johnston, Phys. Rev. B **85**, 214523 (2012).

[38] M. G. Vavilov and A. V. Chubukov, Phys. Rev. B **84**, 214521 (2011).

[39] R. M. Fernandes, M. G. Vavilov, and A. V. Chubukov, Phys. Rev. B **85**, 140512(R) (2012).

[40] E. Berg, S. A. Kivelson, and D. J. Scalapino, Phys. Rev. B **81**, 172504 (2010).

[41] D. S. Inosov, G. Friemel, J. T. Park, A. C. Walters, Y. Texier, Y. Laplace, J. Bobroff, V. Hinkov, D. L. Sun, Y. Liu, R. Khasanov, K. Sedlak, Ph. Bourges, Y. Sidis, A. Ivanov, C. T. Lin, T. Keller, and B. Keimer, Phys. Rev. B **87**, 224425 (2013).

[42] M. N. Gastiasoro, and B. M. Andersen, arXiv:1403.3324.

[43] R. M. Fernandes, L. H. VanBebber, S. Bhattacharya, P. Chandra, V. Keppens, D. Mandrus, M. A. McGuire, B. C. Sales, A. S. Sefat, and J. Schmalian, Phys. Rev. Lett. **105**, 157003 (2010).

[44] M. Yoshizawa, D. Kimura, T. Chiba, A. Ismayil, Y. Nakanishi, K. Kihou, C.-H. Lee, A. Iyo, H. Eisaki, M. Nakajima, and S. Uchida, J. Phys. Soc. Jpn. **81**, 024604 (2012).

[45] H. Kontani, T. Saito, and S. Onari, Phys. Rev. B **84**, 024528 (2011).

[46] R. M. Fernandes, A. E. Böhmer, C. Meingast, and J. Schmalian, Phys. Rev. Lett. **111**, 137001 (2013).

[47] N. Plonka, A. F. Kemper, S. Graser, A. P. Kampf, and T. P. Devereaux, arXiv:1308.6248.

[48] Y. Ran, F. Wang, H. Zhai, A. Vishwanath, and D.-H. Lee, Phys. Rev. B **79**, 014505 (2009).

[49] J. Knolle, I. Eremin, and R. Moessner, Phys. Rev. B **83**, 224503 (2011).

[50] V. Cvetkovic and O. Vafek, arXiv:1304.3723.

[51] R. M. Fernandes, D. K. Pratt, W. Tian, J. Zarestky, A. Kreyssig, S. Nandi, M. G. Kim, A. Thaler, N. Ni, P. C. Canfield, R. J. McQueeney, J. Schmalian, and A. I. Goldman, Phys. Rev. B **81**, 140501(R) (2010).

[52] R. M. Fernandes and J. Schmalian, Phys. Rev. B **82**, 014521 (2010).

[53] A. B. Vorontsov, M. G. Vavilov, and A. V. Chubukov, Phys. Rev. B **79**, 060508(R) (2009).

[54] S. Avci, O. Chmaissem, S. Rosenkranz, J. M. Allred, I. Eremin, A. V. Chubukov, D.-Y. Chung, M. G. Kanatzidis, J.-P. Castellan, J. A. Schlueter, H. Claus, D. D. Khalyavin, P. Manuel, A. Daoud-Aladine, and R. Osborn, arXiv:1303.2647.

[55] E. Hassinger, G. Gredat, F. Valade, S. R. de Cotret, A. Juneau-Fecteau, J.-Ph. Reid, H. Kim, M. A. Tanatar, R. Prozorov, B. Shen, H.-H. Wen, N. Doiron-Leyraud, and L. Taillefer, Phys. Rev. B **86**, 140502 (2012).

[56] J. J. Wu, Jung-Fu Lin, X. C. Wang, Q. Q. Liu, J. L. Zhu, Y. M. Xiao, P. Chow, and Changqing Jin, Proc. Natl. Acad. Sci. U.S.A. **110**, 17263 (2013).